Poincaré Recurrences in Microtron and the Global Critical Structure

B.V. Chirikov[1]

Budker Institute of Nuclear Physics
630090 Novosibirsk, Russia

Abstract

The mechanism of the exponential transient statistics of Poincaré recurrences in the presence of chaos border with its critical structure is studied using two simple models: separatrix map and the kicked rotator ('microtron'). For the exponential transient to exist the two conditions have been shown to be crucial: fast (ballistic) relaxation, and a small measure of the critical structure. The latter was found to include a new peripheral part (halo) of a surprisingly large size. First preliminary empirical evidence is presented for a new regime of Poincaré recurrences including the transition from exponential to exponential statistics.

1 Introduction: exponential vs. power–law PR

As is well known any trajectory of a bounded in phase space motion of Hamiltonian system recurs infinitely many times to some neighborhood of its initial position, for both regular (with discrete spectrum) as well as chaotic (with continuous spectrum) motion. These Poincaré recurrences (PR) do not imply a quasiperiodic motion which is still a widespread delusion (see, e.g., [1]). The difference between regular and chaotic motions lies in the statistics of recurrences which is usually described by the integral distribution $P(\tau)$ that is by the probability for a recurrence time to be larger than τ. In a regular motion such a survival probability $P(\tau)$ has a strict upper bound in τ while for a chaotic motion τ can be arbitrarily long. In both cases PR characterize some fluctuations including arbitrarily large ones in chaotic motion. The PR statistics proved to be a very powerful and reliable method in the studies of chaotic dynamics due to its statistical stability.

[1]Email: chirikov@inp.nsk.su

To my knowledge, such a method was first used (implicitly) in Ref.[2] for the study of a narrow chaotic layer along the separatrix of a nonlinear resonance. The result ($\tau \geq 1$)

$$P(\tau) \approx \frac{1}{\sqrt{\tau}} \tag{1}$$

was a surprise as it contradicted the bounded motion in chaotic layer. Indeed, the total sojourn time $\tau \cdot P(\tau)$ of a trajectory, which is prportional to the measure of the chaotic component of the motion, diverges as $\tau \to \infty$. Later [3], this apparent contradiction has been resolved simply by increasing τ which showed that the exponent of the power–law decay also increased from the initial $\nu = 1/2$ to $\nu \approx 3/2$.

It is instructive to mention that the origin of a short–time computation in Ref.[2] was in apparently reasonable decision to avoid any rounding–off errors by enormous increase of the computation accuracy. As a result, the computation speed, and the available motion time, dropped by several orders of magnitude. Generally, for exponentially unstable (chaotic) motion such an approach is prohibited whatever the computer power. Fortunately, it is also unnecessary for calculating statistical characteristics of the motion like $P(\tau)$ since most of the latter are robust. True, the corresponding Anosov theorem [4] was (and can be so far) proved for the very simple Anosov systems only. Moreover, such a theorem is even wrong for discontinuous (discrete) perturbations like rounding–off ones (see, e.g., Refs.[5]). Nevertheless, all the numerical experience confirms a sort of robustness of the statistical behavior of chaotic systems, at least with some minimal precautions (see, e.g., Refs.[6] for discussion). Notice that without such an 'empirical' robustness the numerical experiments with always *approximate* models would lose any physical meaning!

A power–law decay $P(\tau) \sim \tau^{-\nu}$, whatever the exponent ν, found in [2, 3] for a bounded motion, was at variance with the exponential decay believed to be a generic

case. In Ref.[3] the former was interpreted as a characteristic of a qualitatively new structure of the motion near the chaos border in phase space. Later, it was termed the critical structure, which was described by a renormalization group [7] (see also review [8] and references therein).

Since then, the exponential decay has been considered as a property of ergodic chaotic motion without any chaos borders. However, in recent numerical experiments [9] with an asteroid motion a fairly long transient exponential decay was found. Moreover, it persists in the separatrix map also used, just the same map which seemed to have been well studied in many previous works [3] (see also [8] and references therein).

The main purpose of this paper is to reconsider various regimes of PR, and to formulate the conditions for their realization using two relatively simple models: separatrix and standard maps. Only bounded motion will be considered, with or without chaos borders. First, a classical problem of PR in an ergodic system will be discussed in some details in Section 2. Then, in Section 3, the analysis of various PR regimes in the separatrix map will be presented aimed to resolution of the apparent contradiction mentioned above. In Section 4, PR in the standard map in accelerator (microtron) regime will be described. The latter model presents a unique possibility for quantitative study of the global critical structure. Particularly, a new part of this structure has been found which size was surprisingly large. Finally, in Section 5, the main results of the present study are summarized. In addition, the first preliminary empirical evidence is presented for a new regime of Poincaré recurrences including the transition from exponential to exponential statistics.

2 PR in ergodic system: standard map

Consider, first, an elementary example of 1D homogeneous diffusion in momentum p. It can be described by a Gaussian distribution function

$$f_G(p,t) \,=\, \frac{\exp\left(-\frac{p^2}{2tD}\right)}{\sqrt{2\pi tD}} \tag{2}$$

where $D =< (\Delta p)^2 > /t$ is the diffusion rate. Derivative $f_P(p,t) = df_G/dp$ with boundary condition $f_P(0,t) = 0$ which obeys the same diffusion equation

$$\frac{\partial f}{\partial t} \,=\, \frac{D}{2}\cdot\frac{\partial^2 f}{\partial p^2} \tag{3}$$

describes, then, PR to $p = 0$. The distribution of recurrence times (1) is simply related to an auxiliary function f_G by

$$P(\tau) \,=\, -\,A\int_0^\infty f_P(p,\tau)\,dp \,=\, Af_G(0,\tau) \,=\, \frac{A}{\sqrt{2\pi\tau D}} \,\approx\, \sqrt{\frac{\tau_0}{\tau \,+\, \tau_0}} \tag{4}$$

Here A is normalizing factor, and parameter τ_0 provides a necessary truncation of the preceding diverging expression at small τ. It characterizes the dynamical time scale of the diffusion (cf., e.g., free path in molecular diffusion). If the motion in p is actually bounded (see below), Eq.(4) describes initial free diffusion.

2.1 A little of theory

Now, consider in more details another simple model – the kicked rotator – described by the so–called standard map:

$$\begin{array}{l} \overline{p} \,=\, p \,+\, K\,\sin x \pmod L \\ \overline{x} \,=\, x \,+\, \overline{p} \,-\, p_0 \end{array} \tag{5}$$

on a torus ($0 \le x < 2\pi\,,\ 0 \le p < L = 2\pi n,\ n = 1, 2, ...$).

We seek a solution $f(p,t)$ of diffusion equation (3) with the boudary condition

$$f(0\,,t) \,=\, 0 \tag{6}$$

which provides a loss of probability because of PR to $p = 0$ (and to $p = L$). The orthogonal and normalized eigenfunctions of the diffusion equation for this problem have the form ($k \geq 1$ is integer)

$$g_k(p) \,=\, \sqrt{\frac{2}{L}}\,\sin\left(\frac{\pi k p}{L}\right) \tag{7}$$

with the corresponding eigenvalues

$$\gamma_k \,=\, \left(\frac{\pi k}{L}\right)^2 \cdot \frac{D}{2} \tag{8}$$

which describe the decay rate of the eigenmodes (7). In Eq.(8) the diffusion rate is

$$D(K) \,=\, \frac{K^2}{2} \cdot C(K) \tag{9}$$

with the dynamical correlation function [10]

$$C(K) \,\approx\, 1 \,-\, 2J_2(K) \,+\, 2J_2^2(K) \tag{10}$$

where $J_2(K)$ is the Bessel function.

The set of eigenfunctions (7) and eigenvalues (8) provides a general solution of the diffusion equation with boundary condition (6) for an arbitrary initial distribution $f_0(p) = f(p, 0)$. Peculiarity of PR statistics $P(\tau)$ is just in a very particular initial condition. Specifically, for a single trajectory in numerical experiments the recurrence time τ is determined by the two successive crossings of the *exit line* which is, in the model under consideration, $p = 0 \bmod L$. Hence, the initial distribution is concentrated right here: $|p| \leq K$. The condition for a trajectory with initial $p > 0$ to cross the exit line reads: $p + K \cdot \sin x < 0$. Whence, the probability of crossing is proportional to $\arccos\,(p/K)$, and the normalized initial distribution can be taken in the form:

$$f_0\left(\frac{p}{K}\right) \,=\, \arccos\left(\frac{p}{K}\right), \quad 0 \,<\, p \,\leq K \,<\, L \tag{11}$$

An example of f_0 is shown in the insert to Fig.1. It is convenient to chose $f_0(p)$ on the one side of the exit line which is possible due to the symmetry of eigenfunctions (7).

The difficulty with such an initial condition is in its narrow width which is always comparable with the dynamical scale (both are $\sim K$, a single kick). This violates the diffusion approximation for the exact integro–differential kinetic equation. A simple remedy is well known, for example, from the theory of neutron diffusion where the dynamical scale is the transport free path l_n (see, e.g., Refs.[11] and [1], p.689). A simple correction improving the diffusion approximation amounts to a relatively small shift of the boundary condition (6) from $p_b = 0$ to $p_b = -\alpha l$ where l is the dynamical scale in our problem, and $\alpha \sim 1$ is unknown numerical factor to be determined below from the numerical experiments. This implies an increase of the global scale: $L = L_0 + 2\alpha l$ while the initial distribution remains unchanged as it is obtained directly from the dynamics (5). Notice the corresponding change in eigenfunctions (7).

The general solution of the diffusion problem is given by

$$f(p\,,t) \;=\; \sum_{k=1}^{\infty} f_k \cdot g_k(p) \cdot \mathrm{e}^{-\gamma_k\, t} \tag{12}$$

where the expansion coefficients f_k are determined by the initial condition (11):

$$f_k \;=\; \int_0^K \frac{dp}{K}\sqrt{\frac{2}{L}}\,\sin\left(\frac{\pi k K}{L}\left(\frac{p}{K}\;+\;\Lambda\right)\right)\cdot\arccos\left(\frac{p}{K}\right)\;=$$
$$\sqrt{\frac{\pi}{2L}}\cdot\frac{\cos\left(sk\Lambda\right)\cdot\left(1\;-\;\mathrm{J}_0(sk)\right)\;+\;\sin\left(sk\Lambda\right)\cdot\mathrm{H}_0(sk)}{sk}\;\approx$$
$$\frac{\pi sk}{4\sqrt{2L}}\left(1\;+\;\frac{8\Lambda}{\pi}\right)\cdot\Big(1\;+\;\mathcal{O}(s^2k^2)\Big) \tag{13}$$

Here H_0 is the Struve function, $\Lambda = \alpha l/K \sim 1$ (see below), and $s = \pi K/L \ll 1$ is a small diffusion parameter. The latter approximate expression in (13) holds true for $sk \lesssim 1$.

Now, the PR statistics is described by

$$P(\tau) \,=\, \int_0^L f(p,\tau)\, dp \,=\, \sum_{k=1}^{\infty} f_k\, \mathrm{e}^{-\gamma_k \tau} \sqrt{\frac{2}{L}} \int_0^L \sin\left(\frac{\pi k p}{L}\right) dp \,=$$

$$=\, \frac{2}{\pi}\sqrt{2L} \sum_{m=1}^{\infty} \frac{f_k}{k} \mathrm{e}^{-\gamma_k \tau} \tag{14}$$

with $k = 2m - 1$ because only odd modes contribute to the integral.

Asymptotically, as $\tau \to \infty$, PR decay exponentially (Poisson statistics)

$$P(\tau) \,\to\, \frac{s}{2} \cdot \left(1 \,+\, \frac{8\Lambda}{\pi}\right) \cdot \mathrm{e}^{-\gamma_1 \tau} \,=\, F_1 \cdot \mathrm{e}^{-\gamma_1 \tau} \tag{15}$$

with the characteristic time

$$\tau_1 \,=\, \frac{1}{\gamma_1} \,=\, \frac{2}{\pi^2} \cdot \frac{L^2}{D} \tag{16}$$

which is determined by the first (most slow) mode $m = k = 1$, and which is of the order of the global diffusion time.

The factor F_1 in Eq.(15) characterizes the share of asymptotic exponential decay which is small in the diffusive regime due to $s \ll 1$. The main, initial, decay is a power–law one. Again, due to small s, the sum in Eq.(14) can be approximately replaced by the integral over m to obtain:

$$P(\tau) \,\approx\, \sqrt{\frac{\tau_0}{\tau}} \,\approx\, \sqrt{\frac{\tau_0}{\tau \,+\, \tau_0}} \tag{17}$$

where

$$\tau_0 \,=\, \frac{\pi}{16\, C(K)} \cdot \left(1 \,+\, \frac{8\Lambda}{\pi}\right)^2 \tag{18}$$

function $C(K)$ is given by Eq.(10), and the approximate expression for f_k in Eq.(13) is used. The latter is not applicable for $\tau \to 0$, so that the final expression in Eq.(17) is an approximate truncation of the preceding diverging relation (cf. Eq.(4)).

The power–law/exponential crossover time τ_{cro} is obtained from the comparison of Eqs. (15) and (17), and is given approximately by the relation:

$$\tau_{cro} \approx \frac{L^2}{8\pi D}, \qquad \gamma_1 \tau_{cro} = \frac{\pi}{16} \tag{19}$$

Again, in the diffusive regime ($L^2 \gg D$) the intermediate power–law decay may be very long until the exponential asymptotics is reached.

2.2 Numerical experiments

An example of PR in ergodic case is shown in Fig.1. We use the standard map (5) on a torus of sufficiently large circumference $L \gg K$ to provide a diffusive relaxation ($s \ll 1$, for the opposite limit of ballistic relaxation $s \gtrsim 1$ see Section 4 below). How strange it may seem, the conditions for ergodicity even in such an apparently 'simple' model are still unknown ! However, numerical experiments (see, e.g., Ref.[12] indicate that, at least, for a particular value of the parameter $K = 7$ the share of the regular domains, if any, is negligible ($\lesssim 10^{-9}$) besides the two small islets (per map's period, see Section 4 below). Fortunately, their effect on PR is also negligible because they are related to the accelerator mode in which the momentum p quickly moves around the torus, so that a trajectory immediately crosses the exit line $p = 0 \mod L$ (cf. Section 4).

In Fig.1 empirical data for a particular value of $L = 50\,\pi$ are shown which corresponds to 25 periods of map (5) in p. All the data were obtained from the run of a single trajectory over 10^7 iterations. Transition from a power law (straight dashed line) to an exponential (dashed curve) is clearly seen.

For a quantitative comparison with the theory above (Section 2.1) we fix the dynamical parameter $l \equiv K\sqrt{C(K)} = 12.1$ where the value $C(7) \approx 3$ is used which has been obtained from a special numerical experiment. It considerably differs

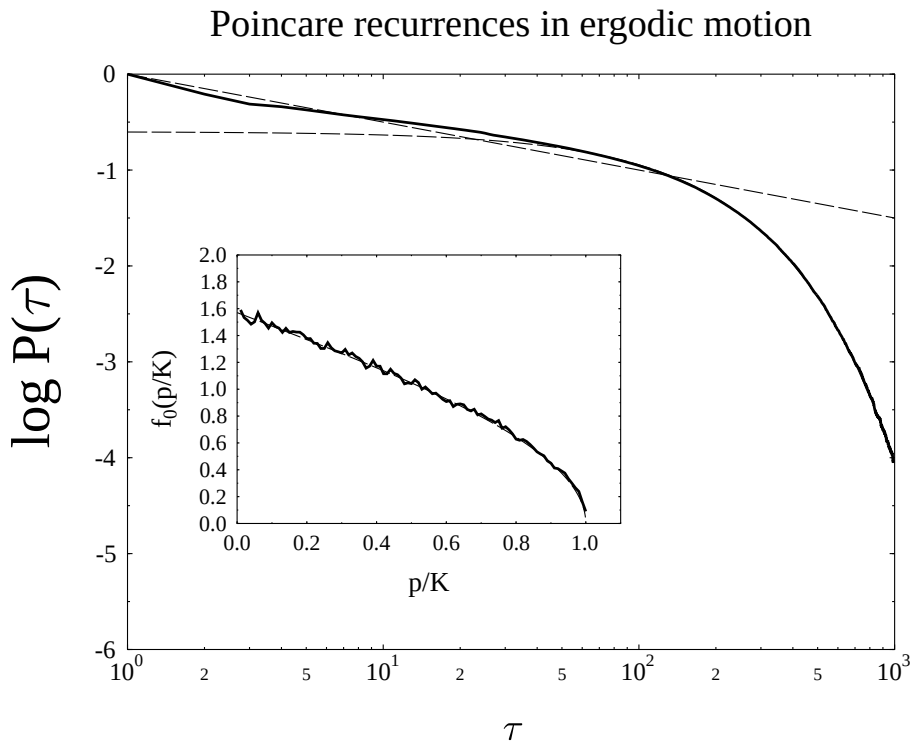

Figure 1: Poincaré recurrences in standard map (5) on a torus with exit line $p = 0 \bmod L = 50\pi$: $K = 7$ ('quasiergodic' motion, see text), $p_0 = 0$, a single trajectory of $t = 10^7$ iterations. Solid line represents numerical data; dashed lines show two asymptotics: a power law (17) (straight line), and exponential (15). Insert: the initial distribution (11), just prior to crossing the exit line. Logarithms here and below are decimal.

from the value $C(7) \approx 1.78$ according to approximate relation (10) just because of accelerator islets mentioned above. Since our model is a map, the minimal empirical recurrence time is $\tau_{em} = 1$ instead of $\tau_{th} = 0$ in a continuous theory (for example, in numerical data $P(1) \equiv 1$). The corresponding corrections are negligible except the initial dependence for $\tau \sim 1$ (see below).

Numerical data in Fig.1 were fitted to Eq.(15) in the interval $\tau = 500 - 1000$ iterations, and the empirical values of the characteristic time $\tau_1 = 125$, and of the factor $F_1 = 0.26$ were obtained. The corresponding values of the correction parameter are $\alpha_\tau = 2.3$, and $\alpha_F = 0.71$. The difference in these two values of α characterizes the accuracy of the correction which is rather poor because of a very narrow initial distribution (see Eq.(11), and discussion around). Without correction ($\alpha = 0$) the theoretical values would be: $\tau_1 = 69$, and $F_1 = 0.07$ which both are substantially underestimated.

For a more systematic study the similar numerical data were computed for a number of L values specified by the integer $n = L_0/2\pi$. The results are shown in Fig.2.

Dependence $\tau_1(n)$ is well described by the uncorrected relation (16) for large n as expected. In intermediate region ($n \sim 3$) the agreement is father improved by the correction which provides a smooth transition to the ballistic limit (see Eqs.(28) and (29) in Section 4). In other words, the correction is not very important for the asymptotic decay rate because it is determined by the first eigenfunction which is only slightly disturbed, for large n, by the shift of the boundary. This is no longer the case for the amplitude F_1 which strongly depends just on the distorted region near the boundary $p = 0$. As a result the correction is most important for large n. The dependence $F_1(n)$ in the intermediate region remains unclear. For $n \gtrsim 10,\ s \lesssim 1/3$

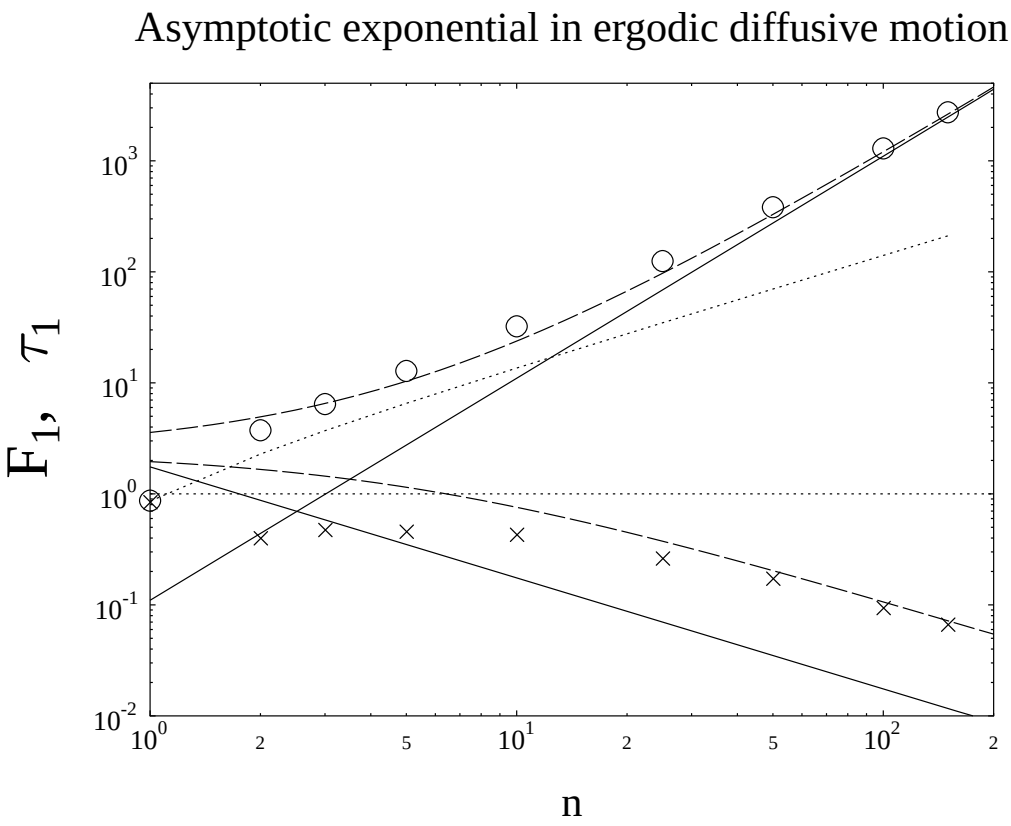

Figure 2: Asymptotic exponential in ergodic diffusive case: numerical values of characteristic decay time τ_1 (16) (circles), and of the factor F_1 in Eq.(15) (crosses) vs. the torus size $n = L_0/2\pi$. Uncorrected dependence is shown by solid straight lines which are transformed into dashed lines by the correction with the same average $< \alpha >= 1.22$. Two dotted lines represent the theoretical dependence (without any corrections) for the opposite, ballistic, limit, Eqs.(28,29)

both relations, Eqs.(15) and (16), are in a reasonable agreement with the numerical data for the same average value of the correction parameter $< \alpha >= 1.22$.

Coming back to Fig.1, we see that the initial power–law decay is well described by a simple relation (17) with $\tau_0 = 1$ which is shown by the dashed straight line, and which would correspond to $\alpha_0 = 0.66 \approx \alpha_F$.

3 PR with a chaos border: separatrix map

Now we consider an opposite limit of essentially nonergodic system with a large chaos border and the critical structure. As an example we take the separatrix map which was studied in many papers (see, e.g., Refs.[2, 3, 8]), and for which a new regime of PR has been recently observed [9]. The latter was the main motivation for the present studies. We take the separatrix map in the form [9]:

$$\begin{aligned} \overline{p} &= p + \sin x \\ \overline{x} &= x - \lambda \cdot \ln(|\overline{p}|) - p_0 \end{aligned} \tag{20}$$

Here the motion is always strictly confined to the so–called chaotic layer: $|p| \leq p_b(x)$. Previously, the most studied case corresponded to big parameter $\lambda \gg 1$. In this limit $p_b \approx \lambda$, so that the width of the layer (2λ) is much larger than the dynamical scale of the diffusion (a single 'kick') which, for map (20), is unity (cf. Eq.(5)). Besides the critical structure along the two borders, the average diffusion rate within the layer is nearly constant (see Eq.(10)):

$$< D > \approx \frac{< C(\lambda/|p|) >}{2} \approx \frac{1}{2} \tag{21}$$

Hence, the initial decay of PR is a simple power law (1) which was observed, indeed, from the beginning [2, 3] (Section 1). The crossover time to a diferent law is given by a simple diffusion estimate:

$$\tau_{cro} \sim \frac{p_b^2}{D} \sim \lambda^2 \tag{22}$$

Unlike the ergodic case, the asymptotics of PR in the presence of chaos border is also a power law but with a different exponent $\nu \approx 1.5$. This is explained by a very specific critical structure near the border where the diffusion rate rapidly drops. As a result no trajectory can ever reach the exact border, even though it is approaching, from time to time, the border arbitrarily close (see Refs. [3, 8, 13] for details).

An example of this well known behavior is shown in Fig.3 (upper solid curve). A transition between the two different power laws (dashed straight lines) at $\tau \sim 100$ is clearly seen in agreement with estimate (22). There is no sign of any exponential decay. Now, how does it appear in a similar model [9]?

The first observation is that in application to celestial mechanics (dynamics of asteroids) the parameter λ of map (20) is typically rather small: $\lambda \sim 1$ [9]. This drastically changes the structure of the layer. First of all, the layer width is reduced down to the size of a single kick. An example is shown in Fig.4. Hence, the diffusion approximation becomes inapplicable. Instead, the so–called ballistic relaxation comes into play which is much quicker. In other words, a slow diffusive motion from the exit line to a critical structure is replaced now by rapid jumps of a trajectory over the whole layer with some probability to get into the critical structure. Since those jumps are very irregular in a chaotic layer the PR are expected to decay exponentially. This is the case indeed as an example in Fig.3 demonstrates (lower solid curve, $\lambda = 1$). The exponential decay can be intermediate only as the trajectory is evetually captured into the critical structure, and the decay turns to a power law. Generally, the initial part of the power law is an approximate relation in that its exponent is not universal, and is even varying with τ. In the latter example $\nu \approx 1.1$ which is rather different from $\nu \approx 1.5$ for the upper curve in Fig.3.

Another interesting and important question is how long is the intermediate expo-

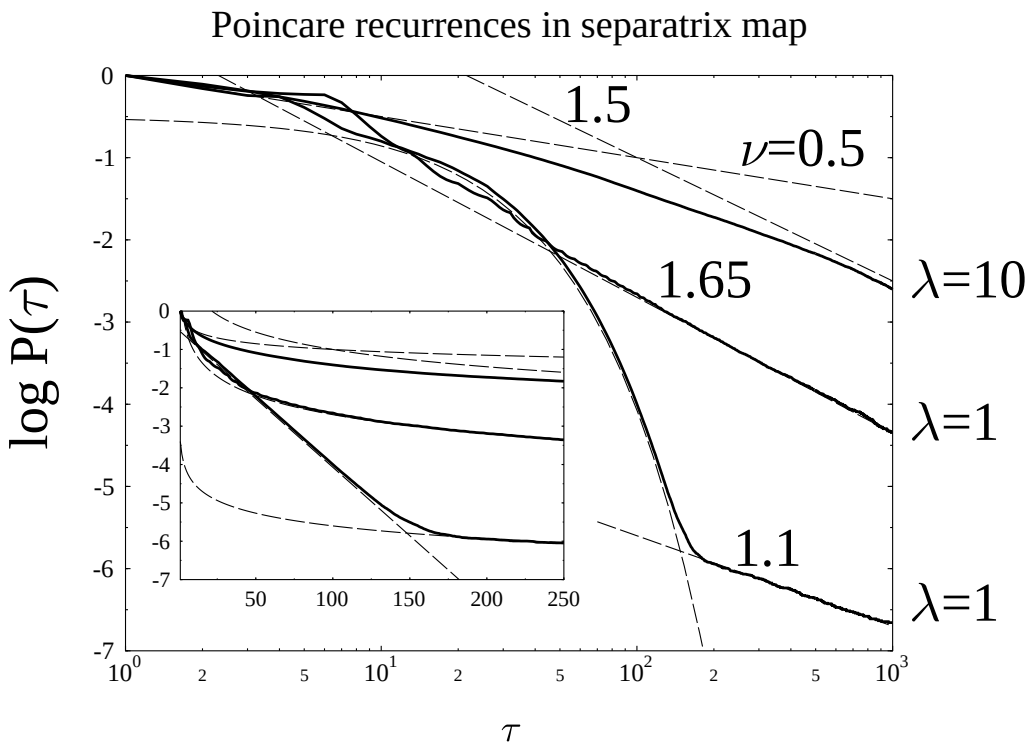

Figure 3: Poincaré recurrences in separatrix map (20): solid lines represent numerical data; straight dashed lines show the power law with the exponents ν indicated nearby; the values of parameter $\lambda = 10$ and 1 are shown at the right; $p_0 = 0$. Two cases with the same $\lambda = 1$ differ by the exit line (see text). Insert: the same in semi–log scale.

nential? For the lower curve in Fig.3 it is rather long: $\tau_{cro} \approx 150$ which corresponds to the PR crossover as low as $P_{cro} \approx 10^{-6}$! However, under different conditions with the same $\lambda = 1$ the exponential is much shorter: $\tau_{cro} \approx 50$, and $P_{cro} \approx 10^{-2}$. The difference is in the exit line as shown in Fig.4.

In the latter case the exit line is usual: $p = 0$. The critical structure is determined by the two big islands comparable in size with that of the whole layer. This entails a rapid capture of a trajectory into the critical structure, and a fast transition to a final power law (with the local exponent $\nu \approx 1.65$). The lower curve in Fig.3 corresponds to the same $\lambda = 1$ but to a different exit line:

$$p_{ex} \; = \; \cos(x) \tag{23}$$

It is chosen in such a way to cut through both stability islands and, thus, to suppress any sticking to their critical structure. Then, the final power law is determined by the critical structure at the layer borders which is apparently very narrow and cannot be discerned 'by eye' in Fig.4. Nevertheless, it does exist as the asymptotic power law of PR in Fig.3 proves. Moreover, the latter even allows us to estimate the size of the critical structure: its relative area (with respect to that of the layer) is $A_{cr} \sim 4 \times 10^{-4}$, or the width $(\Delta p)_{cr} \sim 10^{-3}$ (see Section 4). This exponential transient is well fitted by the relation similar to (15) (up to $\tau \approx \tau_{cro}$) with $\tau_1 \approx 12$, and $F_1 \approx 0.32$. Both values are in a surprisingly well agreement with the uncorrected theory ($\alpha = 0, \; L \approx 4.5$, see Fig.4) which gives $\tau_1 \approx 8.2$, and $F_1 \approx 0.35$. Apparently, this is because the diffusion parameter $s \approx 0.7 \sim 1$ is still not large enough.

Now, we can summarize the conditions for the transient exponential in PR for a nonergodic motion: (i) fast, ballistic, relaxation, and (ii) a small measure of the regular domains. Besides, it turns out that the exponential PR allow for, at least, some estimates of that measure. A more quantitative study of this interesting re-

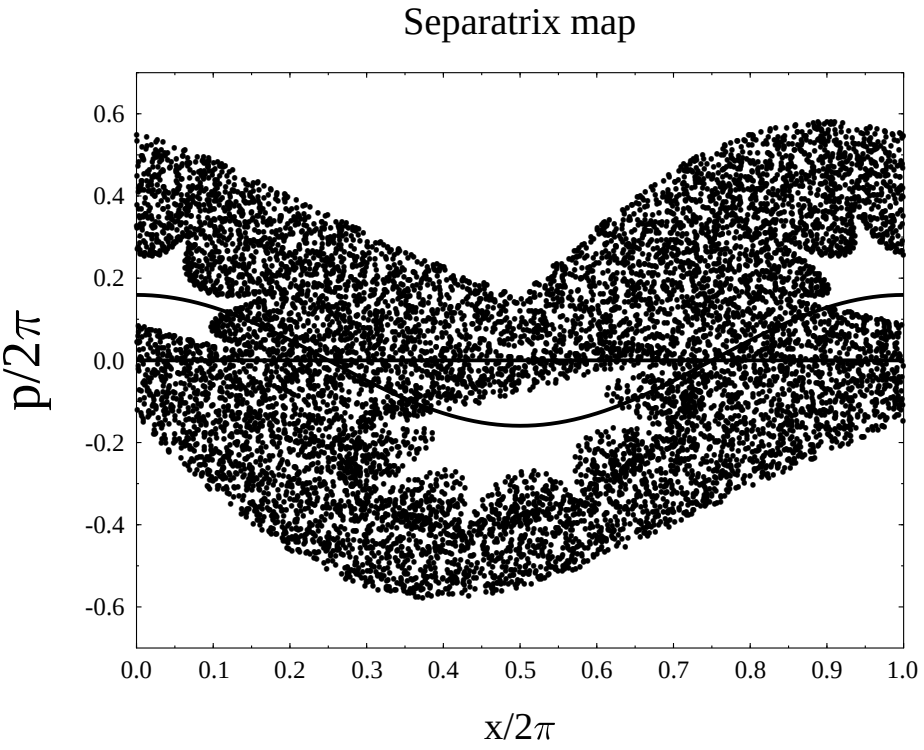

Figure 4: The phase space portrait of separatrix map (20) for $\lambda = 1,\ p_0 = 0$. All points belong to a single trajectory of 10^4 iterations. The straight solid line is the usual exit line $p = 0$ while another one is the special exit line (23) which cuts through the two stability domains and thus blocks the contribution of their big critical structure to PR.

lation is convenient to continue with the standard map again. This is because the latter has an infinite series of the special values of parameter $K = K_n \approx 2\pi n$ for which there are well studied islands of regular motion with a simple scaling and of rapidly decreasing area.

4 PR in microtron: the standard map again

The main advantage of this microtron model is in that it is very simple, especially for numerical experiments, and well studied already. Here we are interested primarily in the domains of regular motion which exist for an infinite series of the special values of parameter $K = K_n \approx 2\pi n$ where $n > 0$ is any integer. Within these domains (islands) $|p|$ grows indefinitly proportional to time which is the so–called microtron acceleration. It was well studied since the celebrated paper due to Veksler in 1944 (see, e.g., [14] and references therein). However, in the present paper, as well as in Ref.[14], the main object for study is not the regular acceleration itself but rather the chaotic motion outside the microtron islands which is generally affected by the critical structure at the island borders. A picture of this scale–invariant border is shown in Fig.5a in dimensionless variables

$$x_s \,=\, (x \,-\, x_0)\cdot K\,, \quad p_s \,=\, (p \,-\, p_0)\cdot K \tag{24}$$

where p_0 is a parameter of map (5), and

$$K\cdot\sin x_0 \,=\, 2\pi n\,, \quad K^2 \,=\, \sigma^2 \,+\, (2\pi n)^2\,, \quad \sigma \,=\, K\cdot\cos x_0\,, \quad -4 \,<\, \sigma \,<\, 0 \tag{25}$$

The latter inequalities determine the stability region around a fixed point $\pm x_0,\ p_0 \bmod 2\pi$. In Fig.5a and below $\sigma = -2$ (the center of stability). For each integer n there are two islets per phase space bin $2\pi \times 2\pi$ one of which is presented

in Fig.5a. The picture shows a single trajectory of 5000 iterations. During this time interval the trajectory is sticking to the critical structure very close to the exact chaos border which results, under particular conditions (see below), in an asymptotic power–law decay of PR (cf. Fig.3 above). The island relative area (with respect to that of the phase–space bin) is given also by a dimensionless relation [14]:

$$A_n \cdot K_n^2 \;=\; A_0(\sigma) \;\approx\; 0.17 \tag{26}$$

where the latter value corresponds to $\sigma = -2$. This area rapidly decreases as island's number n grows. Yet, for any $n \to \infty$ it determines the asymptotic PR decay, as we shall see below.

In Fig.5b another, much smaller, microtron island is shown for comparison. In this case an outside, and much longer, trajectory was used which cannot ever cross the chaos border and enter the island. Its area is given by the same estimate (26) with $A_0(-3.1) \approx 0.0038$.

The main difficulty with the microtron model for our purposes here is the rapid growth in $|p|$ within and around the chaos border. This destroys any long sticking of a trajectory whatever the exit line for PR (cf. Section 3, Fig.4). To overcome this difficulty we used the following method. First, we have chosen the exit line in such a way not to cut any island. It was done simply by fixing parameter $p_0 = \pi(\neq 0 \bmod 2\pi)$ in map (5) without any change in the configuration of map's torus. Second, we compensated acceleration by adding the term $2\pi n$ to the first Eq.(5). This helps, of course, for one island of each pair only.

Now, we need to provide the ballistic regime of relaxation that is a sufficiently large parameter $s = \pi K/L$ (Section 2.1). It is convenient to take $L = 2\pi n$, so that

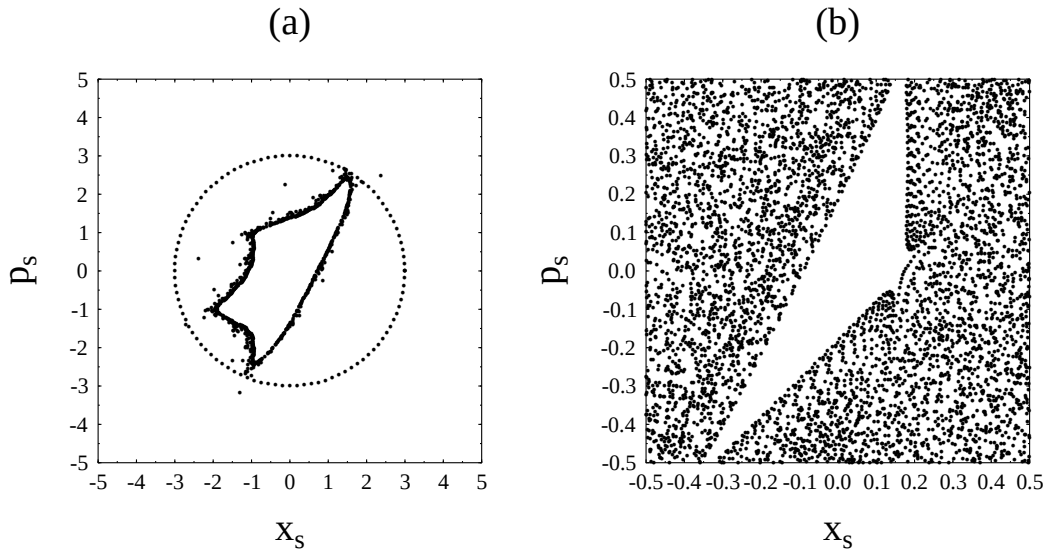

Figure 5: Universal border of microtron islets in scaled variables (24): (a) – in the center of stability interval, $\sigma = -2$, single trajectory of 5000 iterations stuck to the chaos border; (b) – near the edge of stability, $\sigma \approx -3.1$, revealed by an outside trajectory of 10^7 iterations, $K = 7$.

the parameter

$$s \;=\; \frac{\pi K_n}{2\pi n} \;\approx\; \pi \tag{27}$$

is nearly independent of n except a few small values of the latter.

Neglecting any dynamical correlations of the motion (particularly, those caused by the presence of small microtron islets including the compensation of acceleration) it is straightforward to calculate the probability w, per map's iteration, for a trajectory to stay within the torus without crossing the exit line. As is easily verified, it is given by the relation:

$$w \;=\; \int \frac{dx\,dp}{2\pi L/4} \;=\; \frac{2}{\pi L}\int_0^{x_m} dx\,(L \;-\; K\cdot\sin x) \;=\; \frac{2}{\pi}\left(x_m \;-\; \frac{s}{\pi}(1 \;-\; \cos x_m)\right) \;\rightarrow$$

$$1 \;-\; \frac{2}{\pi} \;\approx\; 0.363 \tag{28}$$

where

$$x_m \;=\; \begin{cases} \arcsin\left(\frac{\pi}{s}\right) & , \quad s \geq \pi \\ \pi/2 & , \quad s \leq \pi \end{cases} \tag{29}$$

These general relations were used in Section 2.2 (Fig.2) to draw the ballistic approximation.

The latter expression in Eq.(28) corresponds to the value $s = \pi$ used in numerical experiments. Without additional shift $\Delta p = 2\pi n$ discussed above the average time of the exponential decay would be

$$< \tau > = \; -\frac{1}{\ln w} \;\rightarrow\; 0.988 \tag{30}$$

For $s = \pi$ the shift increases w and $< \tau >$ up to

$$\tilde{w} \;=\; \frac{w}{2} \;+\; \frac{1}{2} \;=\; 1 \;-\; \frac{1}{\pi} \;\approx\; 0.682$$

$$< \tilde{\tau} > \;=\; -\frac{1}{\ln \tilde{w}} \;\approx\; 2.61 \tag{31}$$

Now we can turn to numerical experiments with this microtron model.

4.1 PR in microtron: numerics

The main results of numerical experiments are presented in Fig.6, and in the Table below. In Fig.6 the points show numerical data computed from a single trajectory (for each n) up to 3×10^{11} iterations (for the largest $n = 5000$). The straight solid line is the fitted intermediate exponential with the decay time $< \tilde{\tau} >= 2.41$ in a good agreement with the expected theoretical value 2.61 in Eq.(31). This justifies neglecting dynamical correlations assumed in the above theory in ballistic regime.

The exponential/power–law crossover time systematically increases with n that is with the decrease of the microtron island area (see Table). The power–law tails of PR were fitted by the expression

$$P_n(\tau) \; = \; \frac{A_{cr}(n)}{\tau^{\nu}} \tag{32}$$

Remarkably, all values of the exponent were found to be close: $\nu \approx 2$. The relation of this expression to the size of the critical structure is based on the following hypothesis: dependence (32), fitted to the tail of PR, can be extrapolated back to $\tau = 1$. If true, it allows us to interpret the parameter $A_{cr}(n)$ as the relative area of the whole (global) critical structure around the corresponding microtron island of area A_n.

One could expect that both areas are comparable: $A_{cr}(n) \sim A_n$. Surprisingly, this is not the case (see Table, third column; the data in fourth column will be discussed below). Their ratio $R = A_{cr}/A_n \sim 100$ is not only very large but also slowly increasing with n according to the following approximate empirical relation

$$R(n) \; \approx \; 50\, n^{1/4} \tag{33}$$

The origin of this small correction to a simple scaling $R \approx$ const remains unclear.

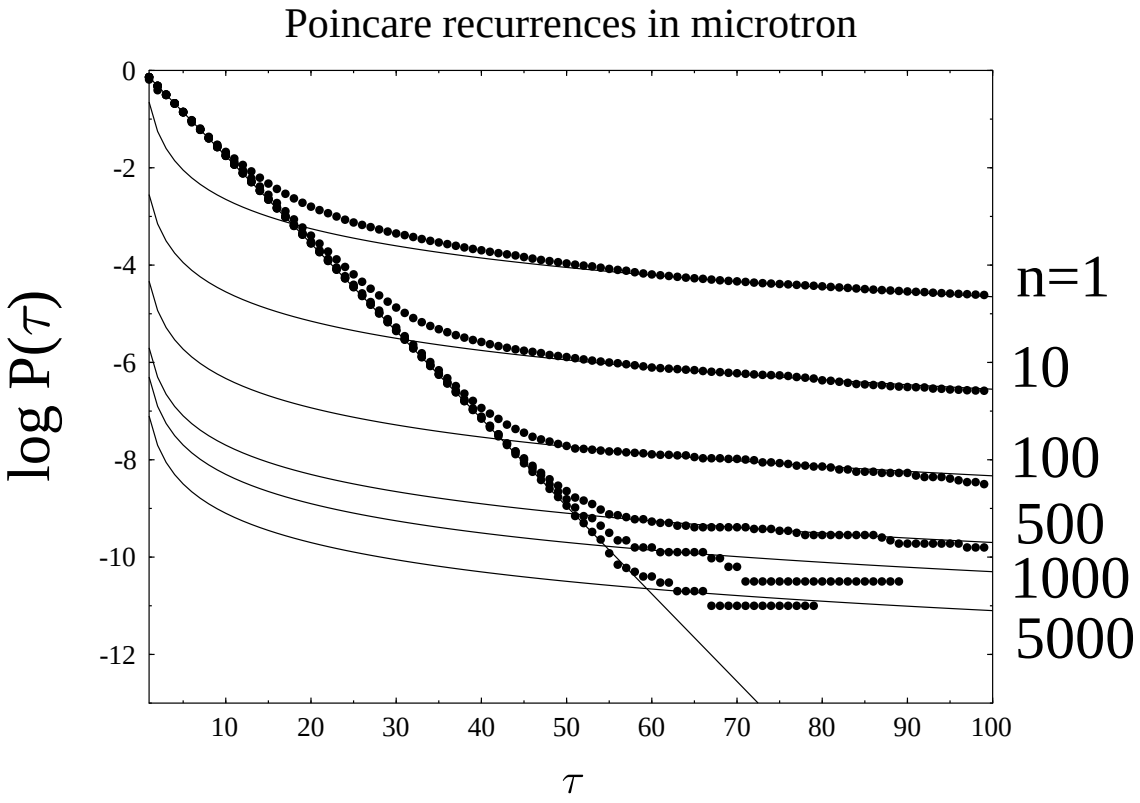

Figure 6: Poincare recurrences in microtron (points) for the values of the microtron parameter n given at the right. Straight line shows the intermediate exponential with the fitted decay time $< \tilde{\tau} >= 2.41$ (cf. Eq.(31)). Solid curves give the fit of asymptotic power law (32) with nearly the same exponent $\nu \approx 2$ extrapolated back to $\tau = 1$ (see text).

Table. Global critical structure around microtron islets

n islet number	A_n islet area	R Fig.6	R_{ex} Fig.7
1	4.30×10^{-3}	36	25.0
5	1.71×10^{-4}	124	–
10	4.31×10^{-5}	65	13.9
100	4.31×10^{-7}	202	10.6
500	1.72×10^{-8}	291	–
1000	4.31×10^{-9}	176	9.8
5000	1.72×10^{-10}	461	–
10^4	4.31×10^{-11}	–	8.6
10^5	4.31×10^{-13}	–	8.3
10^6	4.31×10^{-15}	–	8.1
10^7	4.31×10^{-17}	–	7.7

In any event, the size of the whole critical structure seems to be much larger than expected. This main outer part of the structure looks ergodic, and forms a sort of halo around the usually narrow inner part with a typical admixture of chaotic and regular components of motion. The former reminds the ergodic critical structure around a parabolic fixed point, that is the limiting case of an island of zero size, studied in Ref.[15]. In a sense, such a halo is some 'hidden' critical structure, without internal chaos borders but with apparently strong correlations in the motion which keep a trajectory within this relatively small domain.

Now, the principal question to be aswered reads: is the observed halo a real physical structure or the result of a wrong interpretation of the empirical data using the above extension hypothesis?

4.2 Exit time statistics

To clarify this question a new series of numerical experiments was undertaken. To this end, the exit times from the halo, instead of recurrences, were measured. Such a method was recently successfully used in the studies of the critical structure in Ref.[16]. In the problem under consideration here the measurement of exit times was organized as follows. A number (typically 100) of trajectories with the initial conditions homogeneously distributed over the circle around a microtron island (see Fig.5a) were run until they leave the interval $(0 < x < \pi)$. The dependence of the average exit time τ_{ex} for a series of the circles with increasing radius ρ_s as a function of the area within a circle $A_s = \pi\rho_s^2$ (in scaled variables (24)) was thus computed. The minimal circle of radius $\rho_s = 3$ touches the island, and comprises the area $A_{min} = 28.3$ while island's area in these units is $A_{sn} = 6.72$, the minimal ratio being $R_{ex} = A_s/A_{sn} = 4.21$.

The main results of this measurement are shown in Fig.7 for 8 different values of parameter n up to $n = 10^7$ with the island area as small as $A_n \approx 4 \times 10^{-17}$! This is completely out of reach for the PR method (cf. Ref.[16]). The difference is in a rather short exit time from the halo, we are interested in, as compared to the long recurrence time on the tail where it is eventually separated from the exponential (Fig.6).

The main result revealed in Fig.7 is a transition between the two different scalings. One, for relatively large τ_{ex}, is the standard critical scaling shown by the dashed line which is the fitting of numerical data to the relation

$$R_{ex}(\tau_{ex}) \approx \frac{R_{ex}(1)}{\tau_{ex}} \tag{34}$$

with $R_{ex}(1) \approx 50$. As expected, this part of the data does not depend on n. More-

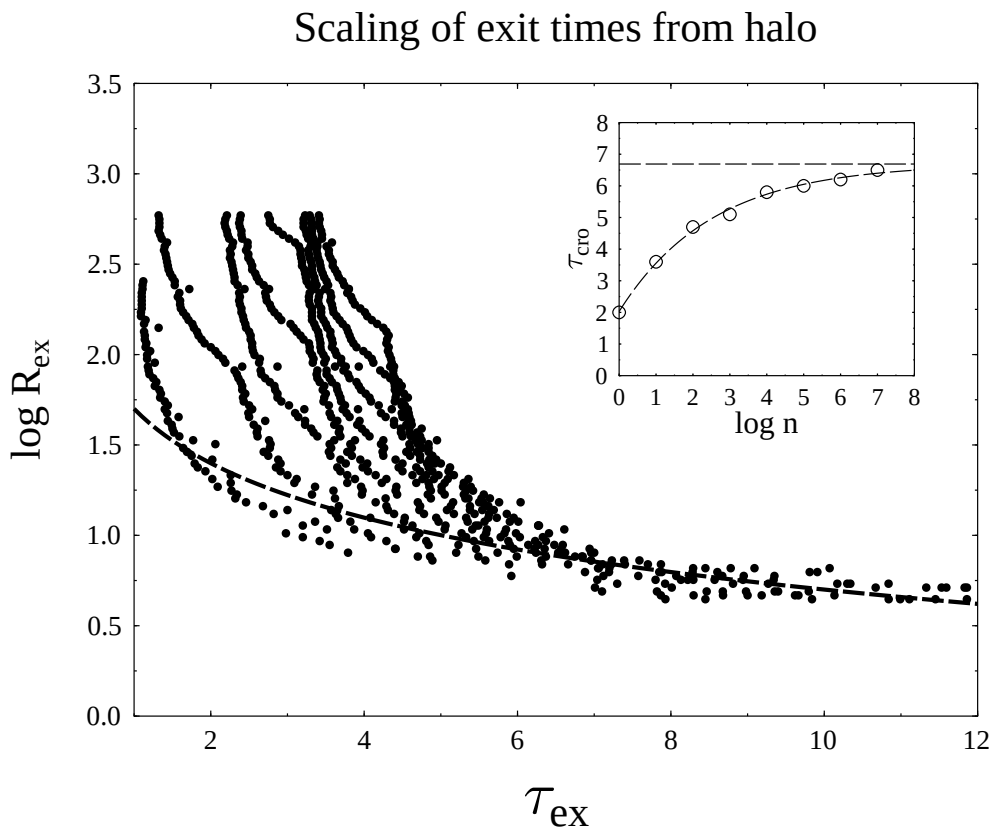

Figure 7: Scaling of exit time from halo: the ratio R_{ex} of the critical to island area vs. the average exit time out of the former (points) from a hundred trajectories (for each of 8 values of n) with initial conditions on a series of circles (see Fig.5a and the text). Dashed line shows the standard critical scaling (34) which breaks down at some values of crossover time τ_{cro} depending on n (insert).

over, scaling (34) is in a good agreement with the PR tail in Fig.6. The relation between the two is well known [3, 8, 14, 16]. Generally, the power–law PR statistics is descibed by (cf. Eq.(32)):

$$P(\tau) \approx \frac{P(1)}{\tau^{\nu}} \approx A(\tau)\frac{<\tau>}{\tau} \tag{35}$$

where $<\tau>$ is the average PR time, and the latter expression is obtained from the ergodicity within the chaotic component of the motion. Using approximate relation $\tau \approx 2\,\tau_{ex}$ [16] we obtain

$$R_{ex}(1) \approx \frac{A(2)}{A_n} \approx \frac{R}{<\tau>\ 2^{\nu-1}} \tag{36}$$

where $R = A_{cr}/A_n \approx A(1)/A_n$ (see above). For integer map's time

$$<\tau> = \sum_{\tau=1}^{\infty} \tau \left(\frac{1}{\tau^{\nu}} - \frac{1}{(\tau+1)^{\nu}} \right) = \zeta(\nu) \tag{37}$$

where ζ is the Riemann function. Whence, for $\nu = 2$ the relation (36) gives (see Eq.(34))

$$R \approx \frac{\pi^2}{3} R_{ex}(1) \approx 160 \tag{38}$$

which is in a reasonable agreement with numerical data (third column in Table). However, unlike the data in Fig.6 where the actual power–law scaling is not seen under much larger exponential transient, the data in Fig.7 clearly demonstrate that the critical scaling does not reach the limit $\tau = 1$ assumed above. Moreover, the crossover time τ_{cro} increases, and hence the size of the global critical structure (R_{ex}) decreases, as n grows (Fig.7, insert). The increase of τ_{cro} must have an upper bound because otherwise the critical structure near the chaos border would be also destroyed in contradiction to the detailed studies of that in anomalous diffusion [14]. Indeed, the empirical dependence τ_{cro} in Fig.7 (insert) can be fitted reasonably well

by the expression

$$\tau_{cro} \;=\; 6.69 \;-\; \frac{4.66}{n^{0.172}} \tag{39}$$

The upper limit in τ_{cro} corresponds, according to Eq.(34), to the lower limit in the ratio $R_{ex} > 7.47$. Combining Eqs. (34) and (39) we obtain approximately

$$R_{ex}(n) \;\approx\; \frac{R_{ex}(1)}{\tau_{cro}(n)} \tag{40}$$

The empirical values of this dependence are given in Table (fourth column). They indicate much smaller, yet still a fairly large, size of the critical structure as compared to the limiting estimate for PR (third column). The former seems to be more reliable and realistic. A different, new and unknown, scaling in Fig.7 for $\tau_{ex} < \tau_{cro}$ requires further studies. What is of importance here is the termination of the critical scaling at a finite $\tau_{ex} = \tau_{cro}$. This determines the outer border of the critical structure.

5 Discussion: a new puzzle

The original motivation of these studies was the unusual exponential transient observed in PR in the presence of chaos border [9]. However, in the course of investigating the mechanism and conditions of this phenomenon a more interesting observation has come out. It suggests the existence of a new, unknown to my knowledge, part of the critical structure surrounding, like a halo, the well–known inner part close to the chaos border. In spite of some contradictory empirical evidence the halo apparently occupies the most of the global critical structure. In any event, in the microtron model considered in this paper the area of the halo is much larger than that of the regular island inside it, even according to the minimal estimates (see Table and Fig.7).

As is well known, the scaling of the peripheral part of the critical structure is

generally nonuniversal, at least quantitatively, in the sense of the corresponding power–law exponents, for example [16]. However, it might be nevertheless typical qualitatively as it appears in our model. In this respect, it would be interesting to look at different examples of the global crtical structure. One possibility is to use the same model with a fixed parameter $L = 2\pi n$ (Section 4) but for different values of the stability parameter σ in Eq.(25). First preliminary numerical experiments have been done for 9 values of σ within the whole stability interval ($-4 \leq \sigma \leq 0$; $2\pi \leq K \leq 7.45$) including the 'quasiergodic' case $K = 7$ used in Section 2 for other purposes. In all cases but the latter the PR behavior was similar to that in the main series of numerical experiments (Fig.6), at least qualitatively. However, just for $K = 7$ a sudden surprise has emerged which is presented in Fig.8.

In spite of a very long run (10^{11} iterations) no clear sign of the expected power–law decay is seen. A small deviation from the final exponential at the end of the dependence is a typical feature due to a poor statistics (cf., e.g., Fig.6). The first exponential is close to the expected one with the fitted decay time $< \tilde{\tau} >= 2.41$ as compared to the theoretical $< \tilde{\tau} >= 2.38$ (see Section 4). For the second exponential the empirical decay time $< \tilde{\tau} >= 23.1$ is about 10 times longer. This means that a trajectory is kept within (sticks to?) a certain domain but not in a way it does so in the usual critical structure. Moreover, the relative area $A_d \sim 2\times 10^{-4}$ of this peculiar domain, estimated similarly to $A_{cr}(n)$ in Eq.(32), is small and is comparable with that of the island inside (Fig.5b): $A_7 \approx 7.8 \times 10^{-5}$. This island does have a chaos border, yet contrary to usual behavior, it does not produce any appreciable power–law decay of PR. Another preliminary remark is that a more careful inspection of Fig.5b seems to suggest a different, more regular than usual, structure of the chaos border for $K = 7$ (cf. Fig.5a). Certainly, this 'anomaly' deserves further

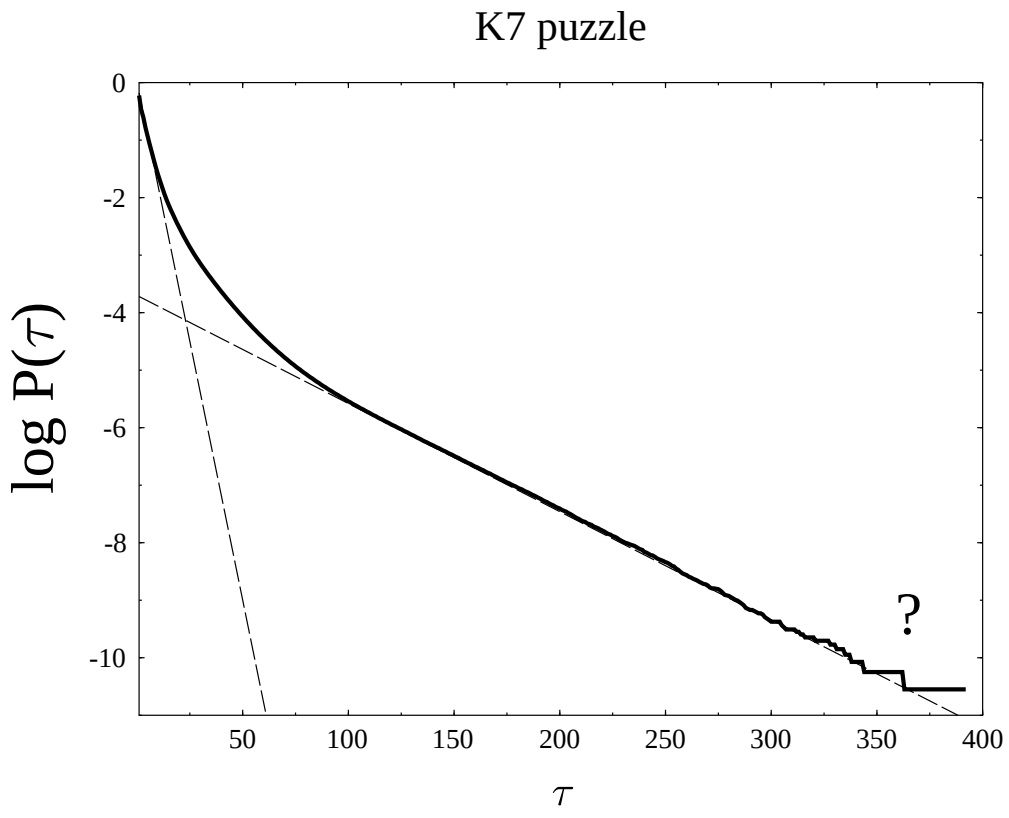

Figure 8: Poincaré recurrences for $L = 2\pi$, and $K = 7$. The solid line shows numerical data from a single trajectory of 10^{11} iterations. Two dashed lines are fitted exponentials with the average decay time $< \tilde{\tau} >= 2.41$, and $< \tilde{\tau} >= 23.1$, respectively.

investigation.

Acknowledgements. I am grateful to I.I. Shevchenko for many interesting discussions and important remarks. This work was partially supported by the Russia Foundation for Fundamental Research, grant 97–01–00865.

References

[1] *Encyclopedia of Physics*, Chief Ed. A.M. Prokhorov, Vol. 1, Ed. D.M. Alekseev, p.345, Soviet Encyclopedia, Moscow, 1988.

[2] S. Channon and J. Lebowitz, Numerical Experiments in Stochasticity and Heteroclinic Oscillation, Ann. N.Y. Academy Sci. **357**, 108 (1980).

[3] B.V. Chirikov and D.L. Shepelyansky, Statistics of Poincaré Recurrences, and the Structure of Stochastic Layer of a Nonlinear Resonance, preprint Budker INP 81–69, Novosibirsk, 1981 (in Russian); Proc. IX Int. Conf. on Nonlinear Oscillations (Kiev 1981), Naukova Dumka **2**, 420 (1984) [English translation: Princeton Univ. Report PPPL-TRANS-133, (1983)]; C. Karney, Physica D **8**, 360 (1983).

[4] D.V. Anosov, Dokl. Akad. Nauk SSSR **145**, 707 (1962).

[5] B.V. Chirikov, Pseudochaos in Statistical Physics, preprint Budker INP 95–99, Novosibirsk, 1995; chao–dyn/9705004; Proc. Intern. Conf. on Nonlinear Dynamics, Chaotic and Complex Systems (Zakopane, 1995), Eds. E. Infeld, R. Zelazny and A. Galkowski, Cambridge Univ. Press, 1997, p.149; B.V. Chirikov and F. Vivaldi, An Algorithmic View of Pseudochaos, preprint Budker INP 98–66, Novosibirsk, 1998; Physica D **129**, 223 (1999).

[6] B.V. Chirikov, Phys. Reports **52**, 263 (1979); B.V. Chirikov, F.M. Izrailev and D.L. Shepelyansky, Sov. Sci. Rev. C **2**, 209 (1981).

[7] R. MacKay, Physica D **7**, 283 (1983).

[8] B.V. Chirikov, Lect. Notes in Physics **179**, 29 (1983); Proc. Intern. Conf. on Plasma Physics (Lausanne, 1984) **2**, 761 (1984); Chaos, Solitons and Fractals **1**, 79 (1991).

[9] I.I. Shevchenko and H. Scholl, Celestial Mech. Dynamical Asron. **68**, 163 (1997); I.I. Shevchenko, Phys. Scripta **57**, 185 (1998).

[10] A. Rechester and R. White, Phys. Rev. Lett. **44**, 1586 (1980); A. Rechester, M. Rosenbluth and R. White, Phys. Rev. A **23**, 2664 (1981).

[11] A.D. Galanin, *The Theory of Nuclear Reactors with Thermal Neutrons*, Glavatom, Moscow, 1959 (in Russian).

[12] G. Casati, G. Maspero and D.L. Shepelyansky, Relaxation Process in a Regime of Quantum Chaos, Phys. Rev. Lett. **82**, 524 (1999).

[13] S. Ruffo and D.L. Shepelyansky, Phys. Rev. Lett. **76**, 3300 (1996).

[14] B.V. Chirikov, Zh. Eksper. Teor. Fiz. **110**, 1174 (1996).

[15] R. Artuso, Correlation Decay and Return Time Statistics, Physica D **131**, 68 (1999).

[16] B.V. Chirikov and D.L. Shepelyansky, Asymptotic Statistics of Poincaré Recurrences in Hamiltonian Systems with Divided Phase Space, Phys. Rev. Lett. **82**, 528 (1999).